QAI LABORATORIES
CERTIFICATION TESTING INSPECTION

1325 N. 108th E. Ave.
Tulsa, OK 74116
918.437.8333 ph. | 918.437.8487 fx.

CLIENT: **PPK, Inc. and PPD, Inc.**
41 Montoya Drive
Branford, CT 06405

Test Report No:	TJ3372	Date:	January 28, 2016

SUBJECT: Evaluation of concrete sealer to assess the impact of the freeze/thaw weathering stress on the concrete fabric within the specimens utilizing petrographic analysis in accordance with ASTM C856.

PRODUCT EVALUATED: Client refers to samples received as **"SingleSeal"**. This project was entered into our receiving system on 7/2/15 in good condition.

TEST REQUESTED: The freeze thaw cycle described on page 2 was developed by QAI Laboratories and the client. Petrographic analysis was performed in accordance with ASTM C856-14 (Standard Practice for the Petrographic Examination of Hardened Concrete).

TEST DATE: November 13, 2015 through December 23, 2015

RESULTS: Results can be found on the following pages.

-

CERTIFICATION: The tests reported here were conducted under the continuous direct supervision of QAI Laboratories Inc., Tulsa, OK. Petrographic analysis, interpretation of results, and formulation of conclusion was performed by Minerology Inc. located at 3321 East 27th Street, Tulsa, Oklahoma 74114 under project number 15394. Results and No revisions of this report will be allowed after 90 days of the original report issue.

Prepared By

Rocky Hale
Materials Test Technician

Signed for and on behalf of
QAI Laboratories, Inc.

J. Brian McDonald
Operations Manager

WWW.QAI.ORG
info@qai.org

Sample Preparation: The specimens consisted of (2) 14” X 14” X 4” concrete slabs on a conditioned soil bed. The soil bed consisted of 1” medium sized gravel and 5” of sandy loam. The concrete mixture used was approximately 1:3 ratio (50 lbs of sand and 17 lbs of portland cement). Type K thermocouples embedded in the slab at depths at 1”, 2”, and 3.5”. Once mixed, poured, and troweled the slabs were allowed to cure for 4 hours at 40°F. Once the cure process was completed one slab was treated with a coat of SingleSeal. The SingleSeal was applied to the test specimen with a common chemical sprayer. The control specimen (no treatment) and test specimen (SingleSeal treated) were conditioned for 4 additional hours at 40°F.

Procedure: Following the curing process the control and test specimens were subjected to environmental cycling consisting of adjusting the temperature to -20°F±2°F for 4 hours and 40°F±2°F for 8 hours. 7 hours and 7-1/2 hours into the 40°F cycle, water was sprayed on the test and control specimens at a rate of 0.5 gpm for 5 minutes. The cycling continued for 20 days.

After the cycling the specimens were removed from the forms and thin sectioned for petrographic analysis in accordance with ASTM C856.

Results Summary: The results of the x-ray diffraction mineralogical analysis (Table I) indicate that the concrete mineralogy is dominated by a mixture of calcite, quartz, and amorphous material. Cement components identified in the XRD evaluation include portlandite, alite, larnite, and ettringite. The amorphous fraction consists of noncrystalline calcium silicate hydrate (CSH) associated with the cement paste materials. The concrete framework is coarse grained, randomly sorted, subrounded, well-graded, and granule and pebble-rich. The aggregate grain components are moderately packed and exhibit common point to point intergranular contacts. The cement paste materials are microcrystalline to very finely crystalline and exhibit locally variable proportions of CSH, intercrystalline microporosity, and partially hydrated cement crystals.

Relative to the control specimen (untreated), the test specimen (treated) is characterized by a relatively large proportion of amorphous CSH within the uppermost 6-7 mm of the concrete profile. The corresponding proportion of partially hydrated and reactive Portland cement crystals (including alite, larnite, and calcium aluminate) is diminished relative to the control specimen (untreated).

The relatively dense & well-hydrated character of the cement paste within the test specimen (relative to the untreated control specimen) has contributed to increased cohesive integrity of the exposure surface. The control specimen exhibits a weblike spatial distribution of (finely dispersed) microfracture intersections which gives the test block a mottled appearance in reflected light. The density of fracture intersections on the exposure surface of the test specimen (treated) appears nominal relative to the untreated sample

The dispersed & diffused character of the fracture distribution in control specimen (relative to the test specimen) is attributed to increased heterogeneity in the strength of the irregularly hydrated cement groundmass. The introduction of the metasilicate curing agent along the surface of the test specimen promoted the interlocking of the cement hydration products (predominantly CSH), thereby favoring the relative ‘armoring’ of the concrete surface and the concentration & growth of relatively localized & elongated fractures oriented subparallel to the slab surface.

X-ray Diffraction: The XRD mineralogical evaluation (Table I) reflects the composition of the concrete substrate within the uppermost 6 mm of the cross section within each of these specimens. The mineralogy of this mix design is dominated by a combination of calcite coupled with significant amounts of quartz, amorphous material, feldspar, and cement paste constituents. The calcite composition is significant within each of these specimens and ranges from 52-55% of the mineral mass. The calcite is present in the form of limestone RFs (rock fragments) within the sand and coarse aggregate fractions of the concrete. Calcite is also present as a replacement for cement paste materials within the near-surface carbonized halo of the concrete. Crystalline mineral phases attributed to the portlandite cement fraction include amorphous material (i.e., non-crystalline calcium silicate hydrate or CSH), portlandite, alite, larnite, and ettringite. Minor amounts of clay matrix minerals are also present and are associated with scattered clay-rich siltstone aggregate particles contained in the mix design.

Table 1

	Sample ID	Test Block #1	Test Block #2
	Lab ID	15394-01	15394-02
Mineral Constituents	Chemical Formula	Relative Abundance (%)	
Quartz	SiO_2	21	18
Albite Feldspar	$(Na,Ca)AlSi_3O_8$	2	2
Microcline Feldspar	$KAlSi_3O_8$	3	4
Calcite	$CaCO_3$	52	55
Portlandite	$Ca(OH)_2$	4	3
Alite	Ca_3SiO_5	3	3
Larnite (Belite)	beta-Ca_2SiO_4	2	3
Ettringite	$Ca_6Al_2(SO_4)_3(OH)_{12} . 25H_2O$	1	1
Clay Minerals / Mica		1	1
Amorphous		11	10
TOTAL		100	100

Thin Section Petrography: The thin section petrographic analysis provides a microscopic evaluation of the mineralogy, texture, and fabric of the concrete in accordance with ASTM C856 (Standard Practice for the Petrographic Examination of Hardened Concrete). Representative photomicrographs for these core samples are provided in Appendix 1. The following discussion highlights the most significant findings of the petrographic analysis.

Core ID	Treated	Untreated
Lab ID	**15394-01**	**15394-02**
ICRI Surface Profile	CSP2	CSP1
Carbonation Depth (mm)	~0.35 mm	~0.40 mm
Water / Cement Ratio	~0.45	~0.45
Air-Entrapment Macroporosity (%)	~4.0%	~3.5%
Fracture Porosity (%)	~1.0 %	~1.2%

Macroscopic Properties: The concrete test samples consist of 14" x 14" x 3.5:" blocks of portland concrete. Cross sections for each of these blocks were polished and evaluated using a reflected light microscope. The concrete framework is characterized as coarse grained, granule and pebble-rich, poorly sorted to very poorly sorted, and subrounded, with common swarms of sub-horizontal microfractures. Aggregate components are moderately packed and exhibit common point to point intergranular contacts. The concrete fabric is moderately porous & contains scattered air-entrapment macropores. No indications of embedded steel are indicated in the cross section prepared for these samples. The ICRI surface profile is estimated to range from a CSP1 to a CSP2 with near-surface carbonation of the cement paste materials estimated to penetrate to a depth of ~0.35-0.4 mm beneath the slab surface. The control specimen exhibits an exposure surface characterized by a relatively dispersed & diffuse distribution of randomly oriented microfractures which have contributed to a mottled and 'crazed' appearance of the concrete surface. Reflected light analysis of the concrete cross sections indicate that sub-horizontal microfracture strain is common with separation planes that preferentially follow the aggregate cement bond lines. No evidence of surface spalling or significant pitting of the concrete surface was evident.

Fabric & Texture: The concrete fabric is grain supported, mildly to moderately packed, with scattered air entrapment macropores. The aggregate grains are very randomly sorted, well graded, and subrounded, with microcrystalline cement paste materials that are typically densely interlocked and well adhered to grain surfaces.

Aggregate: Aggregate materials comprise ~64-68% of the bulk volume within these specimens. The coarse aggregate fraction is dominated by limestone RFs coupled with moderate amounts of chert and quartz-rich granitic RFs. The sand-sized aggregate materials are dominated by medium to coarse grained quartz and feldspar-rich sand containing locally significant amounts of limestone and chert RFs. Minor aggregate types include siltstone and shale RFs. No indications of alkali aggregate corrosion are evident within these test samples.

Pore System: Pore types include common air-entrainment macropores, intercrystalline microporosity (distributed within the cement paste materials), and fracture porosity. The relative proportion of fracture void space is fairly consistent within each of the test blocks and estimated to range from ~1.0-1.3% of the bulk volume.

Concrete Weathering & Cohesive Integrity: The relatively uneven & irregular hydration of the cement paste materials in the control specimen has contributed to the occurrence and distribution of randomly oriented, dispersed microfractures within the cement groundmass of this sample. In contrast, the test specimen exhibits a localized fracture strain that is concentrated along meandering sub-horizontal planes that are stacked within the concrete cross section. The dispersed geometry of the fracture strain within the control specimen is attributed to the (relative) heterogeneity of the paste materials.

Conclusions: The extreme laboratory conditions utilized during the test period are not likely to be observed in the field. No thermal blankets were used during the testing or in conditioning the specimens. Both the test and the control specimens were repeatedly cycled through a temperature range of -20°F to +40°F to simulate multiple extreme freeze/thaw cycles. At the end of each of the thawing cycles and prior to refreezing, water was sprayed on the surface of all specimens to simulate precipitation.

Test Findings:

- There was no evidence found of surface cracking, spalling, or pitting during the duration of the test.
- The control specimen (untreated) showed greater cohesive damage to the concrete framework than did the test specimen (treated with SingleSeal).
- The test specimen (treated with SingleSeal) exhibited strong water retention, which allows for a more consistent internal temperature that is an integral part of the curing process.
- The density of fracture strain intersections of the exposure surface of the test specimen (treated with Single Seal) appears nominal relative to the control specimen (untreated). These fracture strain intersections found in the control specimen (untreated) are likely to contribute to the influx of surface water during thaw cycles, thereby promoting further expansive strain and weakening of the concrete.
- The corresponding proportion of the partially hydrated and reactive cement crystals is significantly diminished in the test specimen (treated with SingleSeal) relative to the control (untreated)
- Throughout the testing process the test specimen (treated with SingleSeal) showed hydrophobic moisture control properties that were not found in the control specimen (see Appendix 3 pictures).

In conclusion, the SingleSeal test specimen, through petrographic analysis, did protect both the surface layer and the internal integrity of the concrete when compared to the control (untreated) specimen. For further detail and clarification, see the test report in its entirety contained herein.

Appendix 1

Test Specimen (Treated) – Macro Picture

<u>Control Specimen (Untreated) – Macro Picture</u>

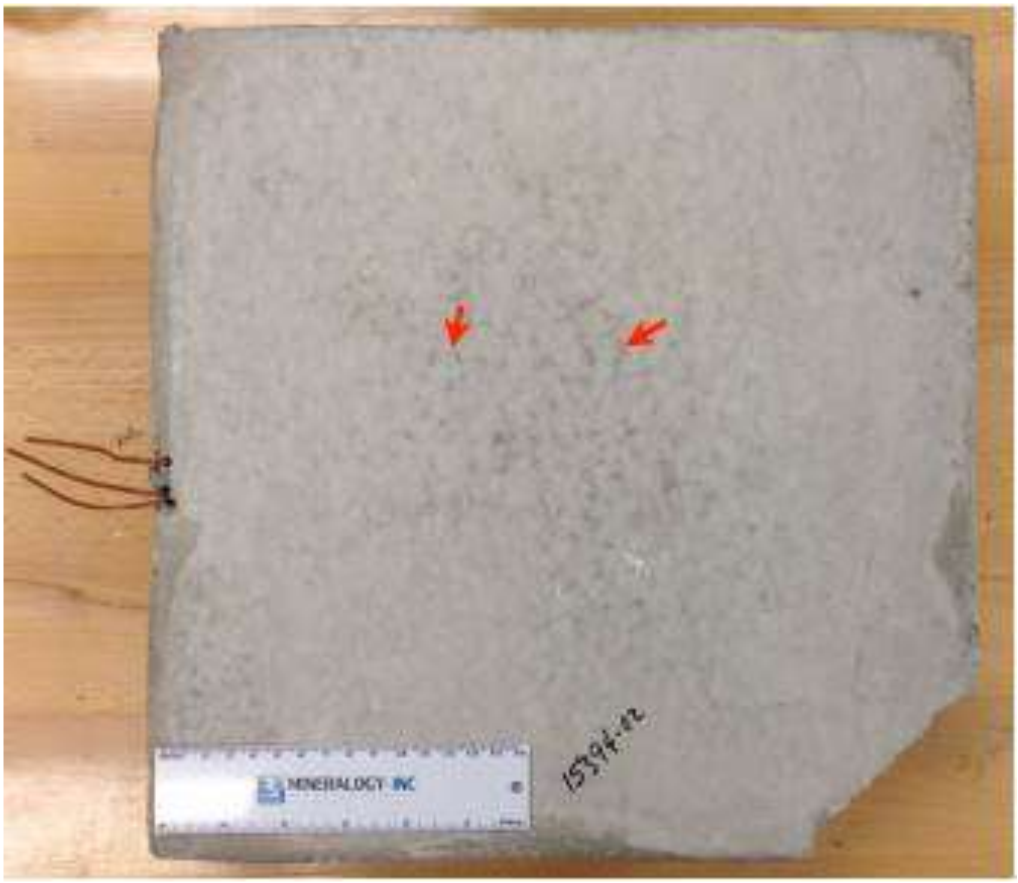

The distribution of the micro-cracks on the surface of the treated sample resembles mud-cracks on a tidal flat (red arrows).

Test Specimen (Treated) – Slab View

Control Specimen (Unreated) – Slab View

Test Specimen (Treated) – Petrographic Thin Section

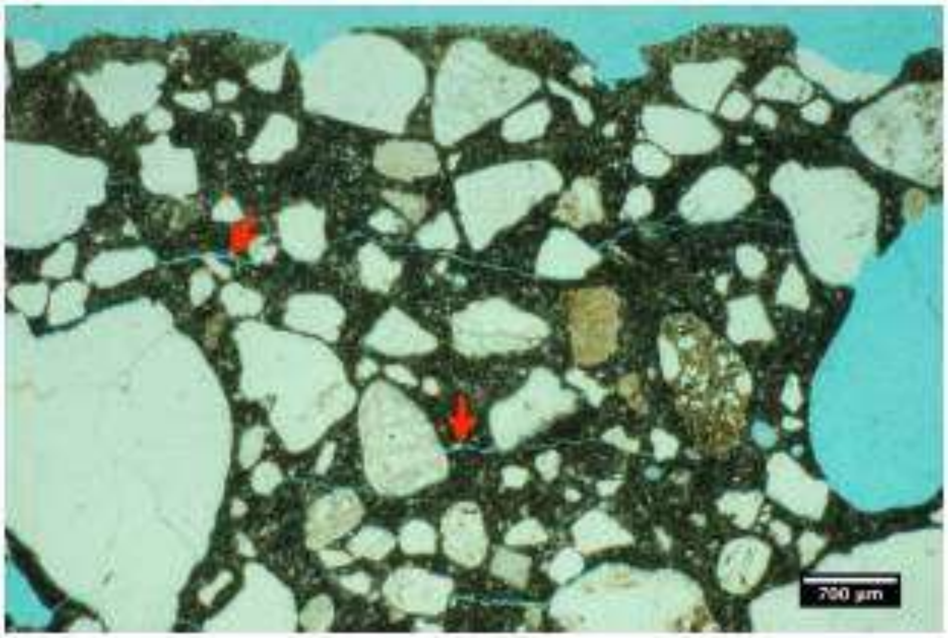

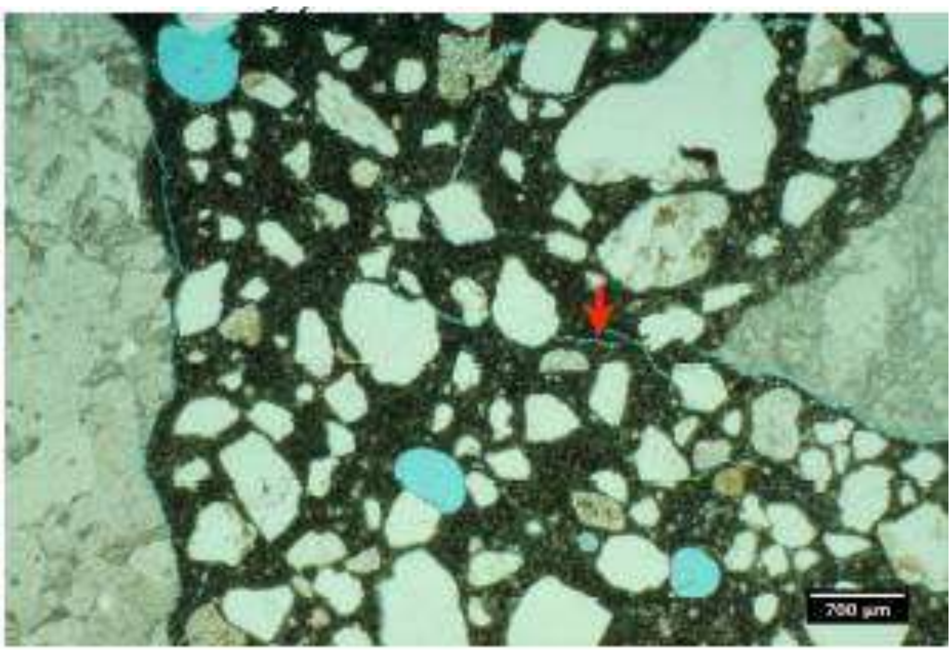

*Fracture stain (blue: red arrows) is attributed to cyclic exposure of the slab to freeze/thaw weathering

Test Specimen (Treated) – Petrographic Thin Section (Continued)

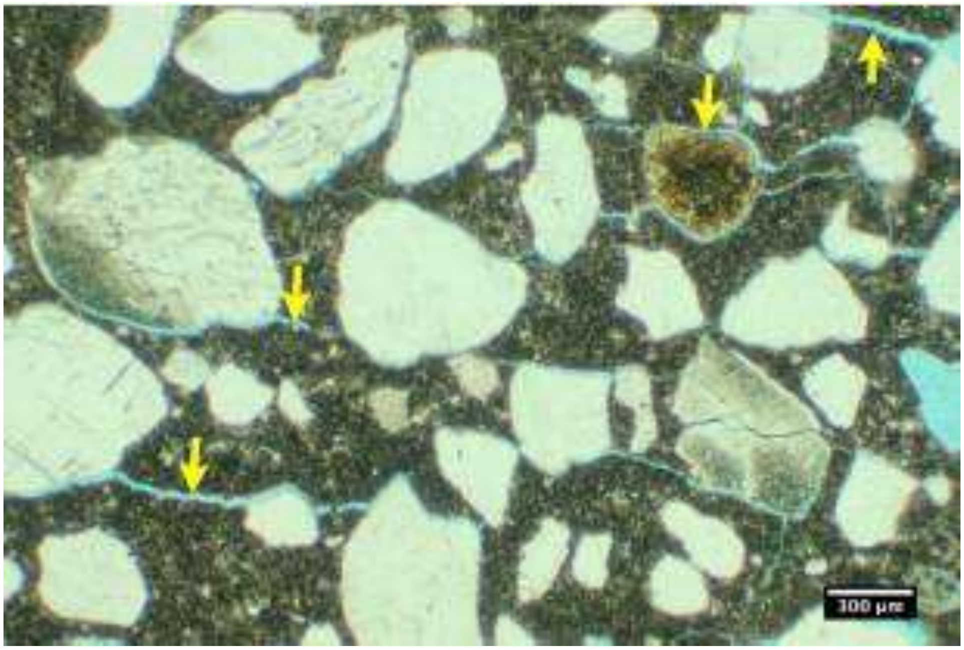

The paste constituents are densely interlocked and well lithified, contributing to the growth of fracture strain sub-parallel to the slab surface (yellow arrows).

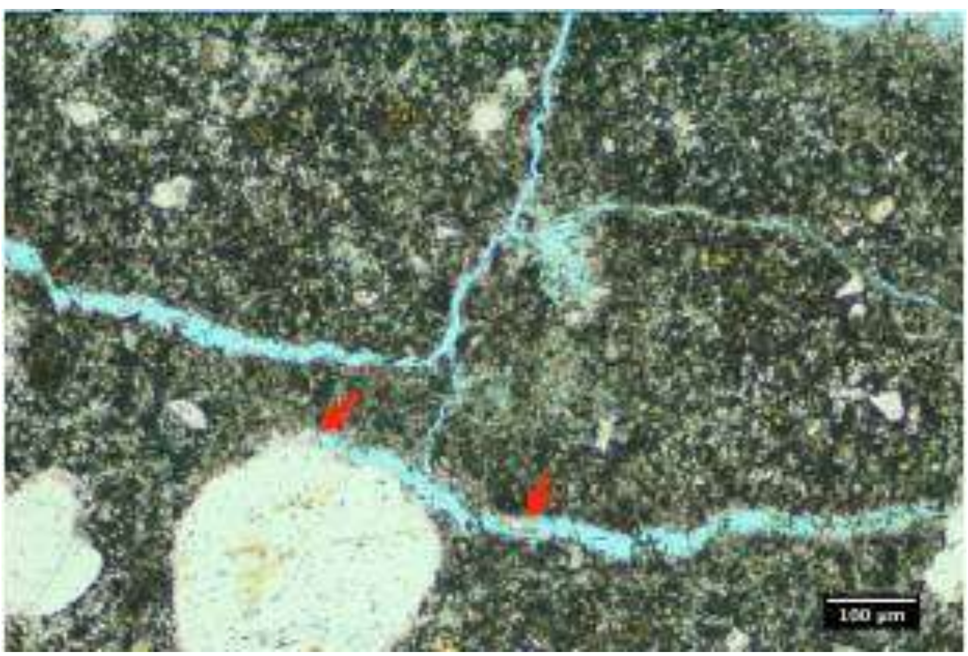

The fractures locally contain traces of authigenic calcite (red arrows) & ettringite

Control Specimen (Untreated) – Petrographic Thin Section

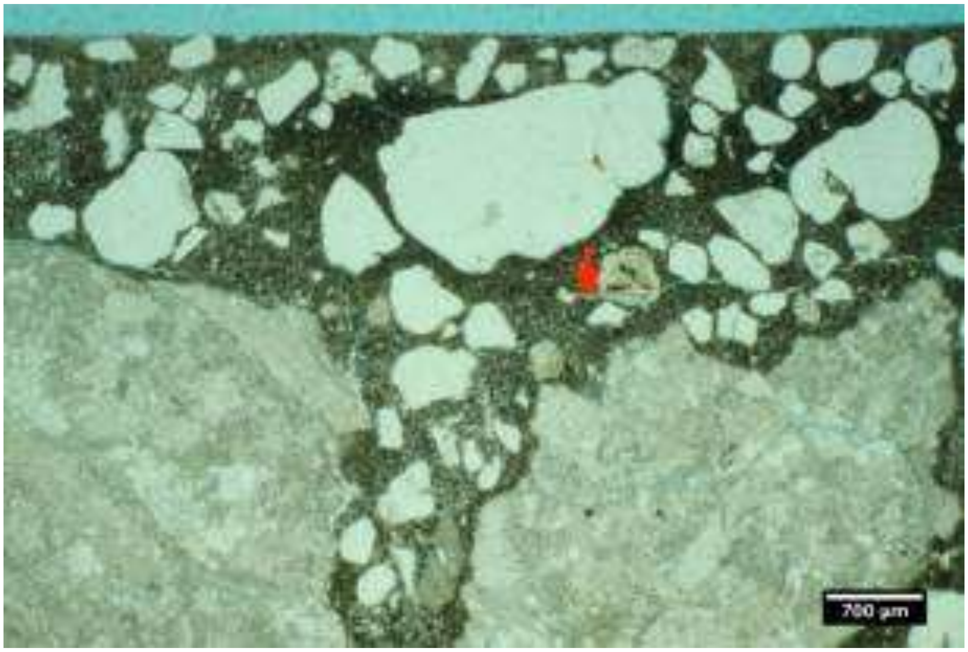

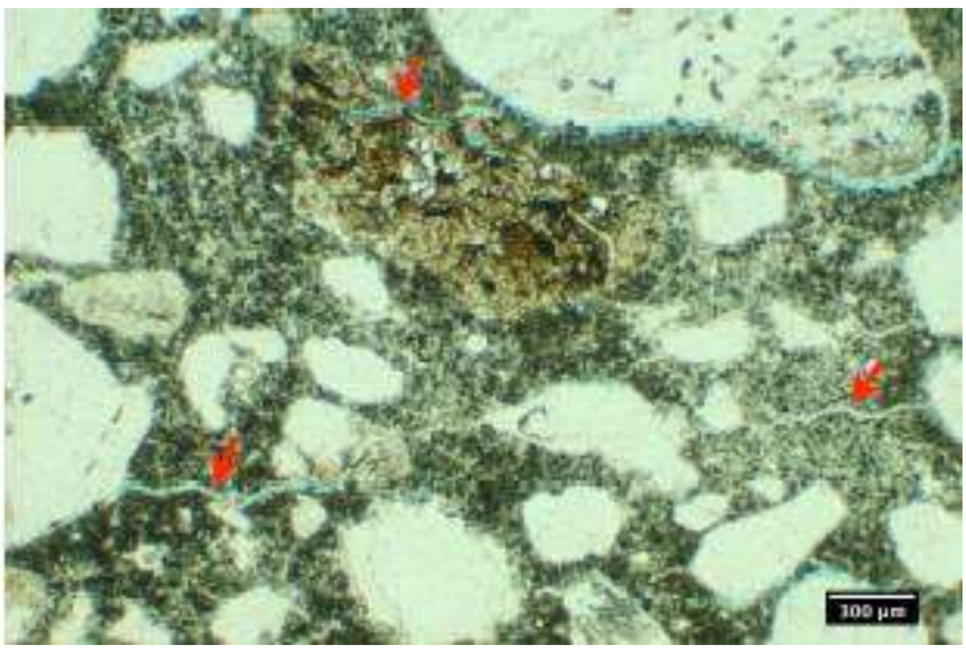

The matrix within the control specimen exhibits a dispersed, braided network of microfractures that have weakened the cohesive integrity (red arrows).

Control Specimen (Untreated) – Petrographic Thin Section (Continued)

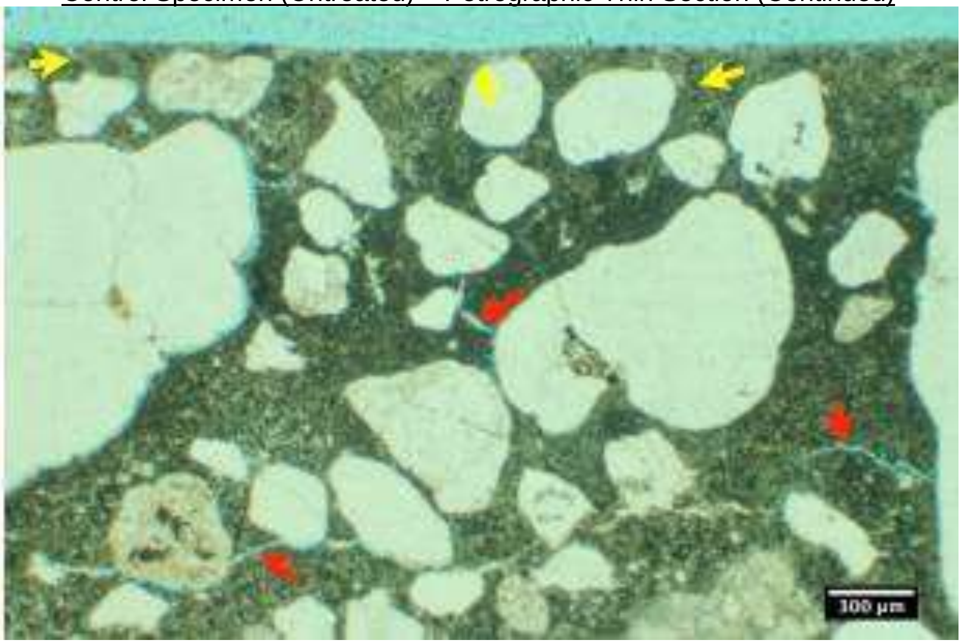

The dispersed geometry of the microfracture network in the un-treated slab has contributed to locally significant weakening of the cohesive integrity (red arrows).

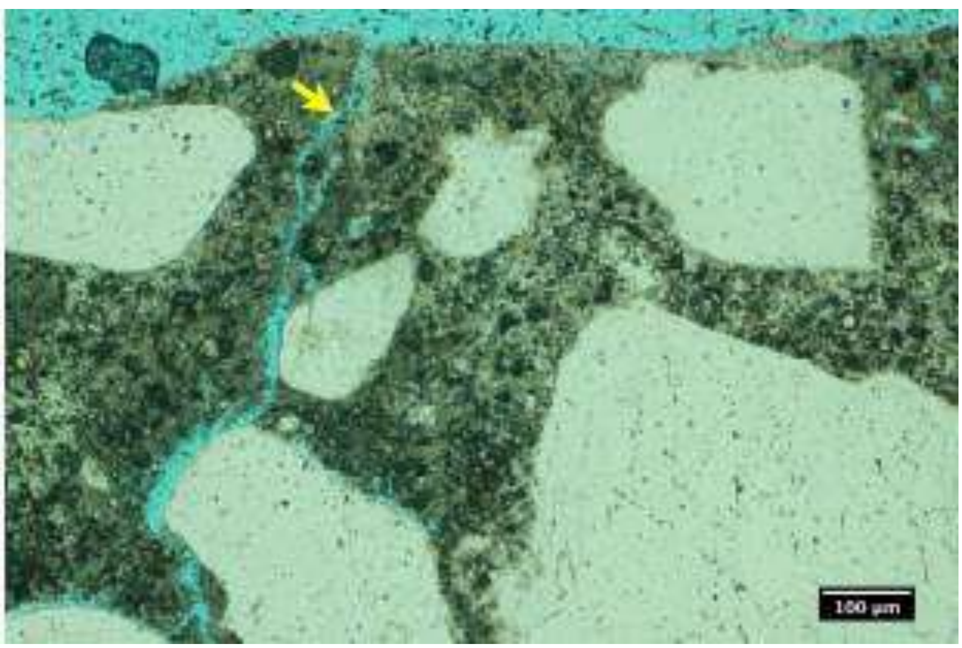

The exposure surface is intersected by an abundance of microfractures (yellow arrows) that expose the framework to H_2O absorption & increased expansive strain.

Control Specimen (Untreated) – Petrographic Thin Section (Continued)

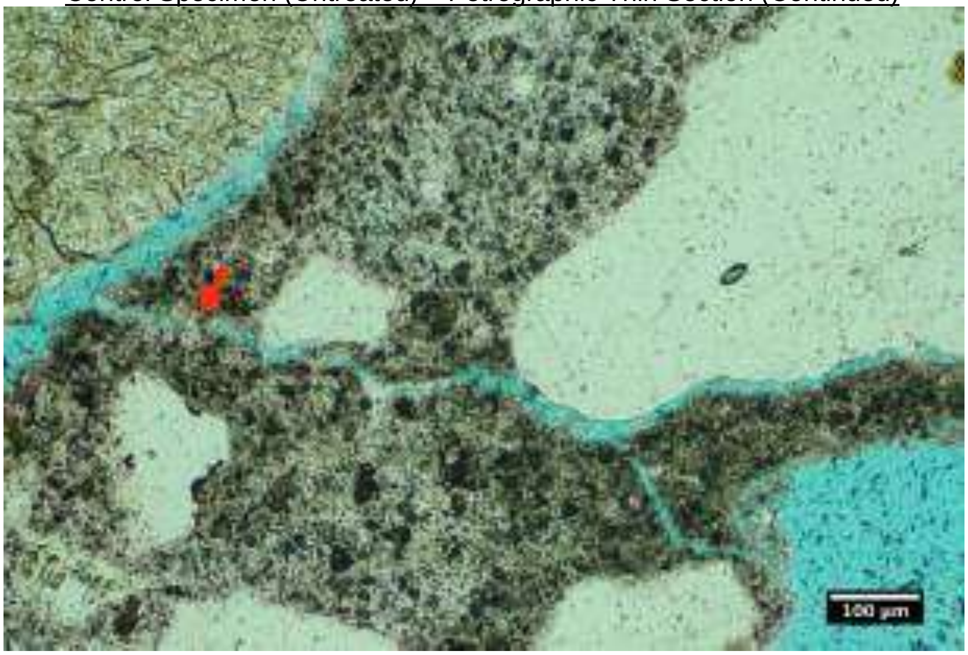

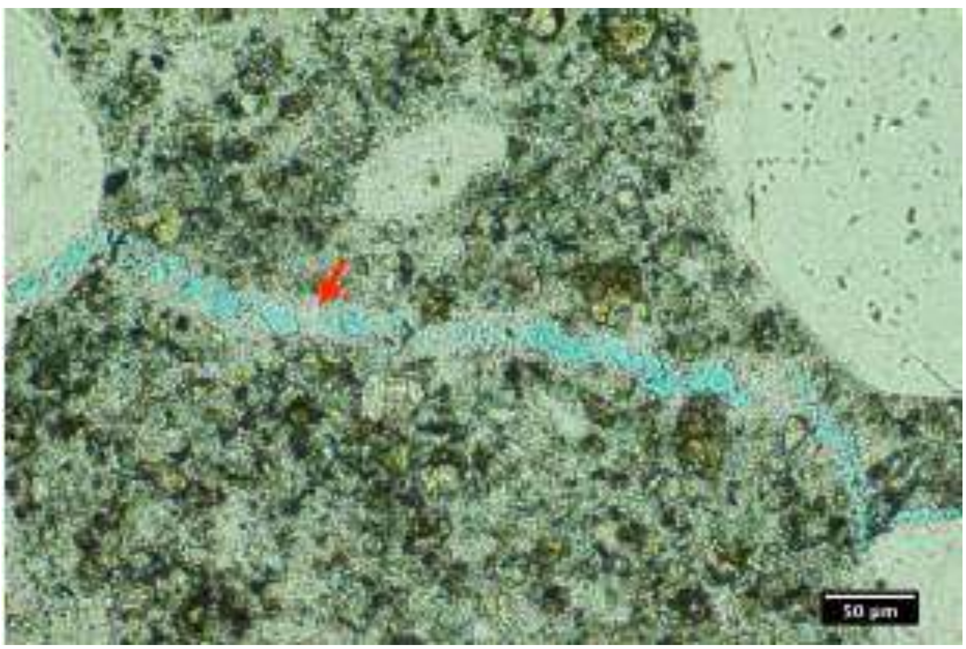

Fracture-bridging calcite cement (red arrows). Note the diffuse & microporous character of the cement paste.

Appendix 2: Temperature

1" Thermocouple Temperatures

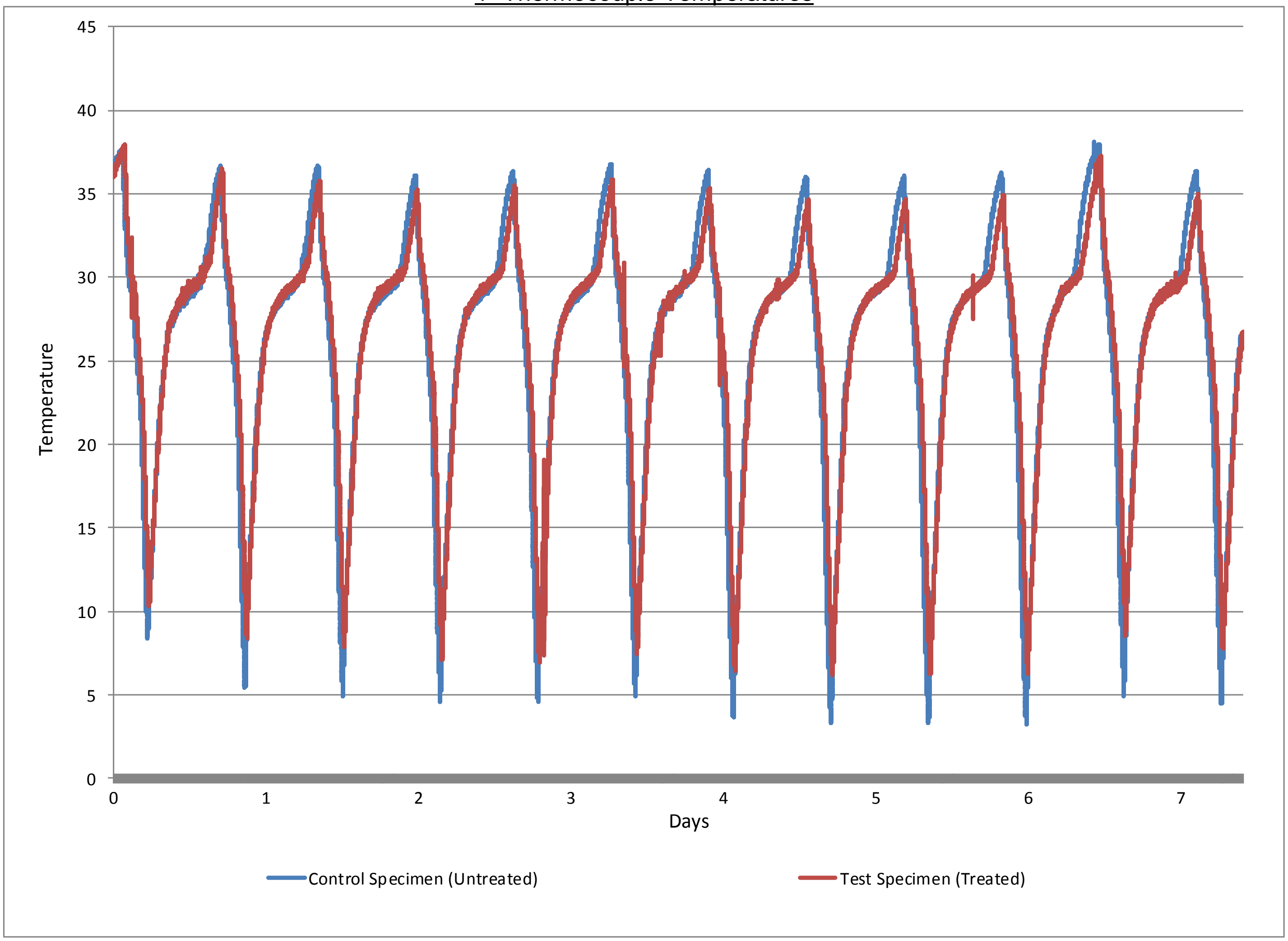

Test specimen has a more consistent internal temperature when compared to the control specimen. The test specimen also demonstrated an average minimum temperature of 4.2°F warmer than the control specimen and

Appendix 3: Weight and Moisture Retention

Weight Loss:

Date	Control Sample (g)	Rate of Loss ($g/m^2/24$)	Test Sample (g)	Rate of Loss ($g/m^2/24$)	Rate Percentage (%) (Control-Test)/Control) * 100
11/13	25424		24423		
11/16	25338	124.84	24347	105.12	15.80
11/17	25312	118.30	24325	97.21	17.83
11/18	25287	113.42	24305	90.86	19.90
11/19	25264	108.11	24286	84.46	21.88
11/20	25241	103.05	24268	78.52	23.81
11/23	25179	89.64	24222	63.34	29.34
11/24	25160	85.57	24209	58.96	31.10
11/25	25143	81.62	24196	54.85	32.80
11/30	25065	64.62	24147	38.30	40.73
12/1	25051	61.66	24139	35.64	42.20
12/2	25038	58.85	24131	33.17	43.64
				Average	**30.57**

Test specimens on average had a 30.57% better water retention rate than the control specimen.

Control Specimen Test Specimen

*The test specimen has evidence of ice and frost on the surface while the control specimen has absorbed the moisture.

***** End of Report *****